IASSNS-HEP-90/75
NYU-NN-90/3
November, 1990

Color coding and its interaction with spatiotemporal processing in the retina*

JOSEPH J. ATICK AND ZHAOPING LI

School of Natural Sciences, Institute for Advanced Study
Princeton, NJ 08540, USA

and

A. NORMAN REDLICH

Department of Physics and Center for Neural Science
New York University
New York, NY 10003, USA

* Work supported in part by a grant from the Seaver Institute.

ABSTRACT

We use the theory of early visual processing proposed in ref. [1] to deduce the color encoding strategies of the retina. The calculated retinal transfer functions display a nontrivial coupling between color and spatiotemporal processing even when the autocorrelator of natural scenes has no coupling between the chromatic and the space-time dimensions. This coupling in the transfer function is fundamentally due to photoreceptor noise, and where red and green cone activities are highly correlated, as they are in humans and monkeys, it leads to the spatio-temporal-chromatic opponent ganglion cells found in primates. Ignoring the blue cones, we find two types of ganglion cells whose receptive field organization is either red center with a green surround or green center with a red surround, as found by Derrington et al. [4] in monkeys. On the other hand, when the correlation between the red and green cone outputs is small, as is the case in shallow fresh water fish, we arrive at the "double opponency" cells observed in goldfish. We also argue that adding blue cones (which are rare) leads to a third type of cell with $R + G - B$ opponency.

1. Introduction

In ref. [1], a computable theory of early visual processing, in particular retinal processing, was proposed. According to this theory, the underlying purpose of retinal encoding is to produce the most "efficient" representation of the information available at the level of the photoreceptors. The measure of efficiency is a generalized redundancy which shows that the sources of inefficiency are correlations and noise in the incoming signal. The retina therefore recodes to eliminate correlations, where correlations are most significant (high signal to noise regime), and to reduce noise in the regime where noise is dominant. This gives a quantitative prediction for the retinal transfer function at any adaptation level. In ref. [2] the predictions for the spatiotemporal processing were quantitatively compared with data from contrast sensitivity experiments. The extent of agreement of the theory with experiment is very encouraging and reinforces the belief that the retina is performing an optimal encoding, an idea that Barlow had suggested many years ago [3].

In this paper, we derive the predictions of the theory of ref. [1,2] for the encoding strategies of the retina when we include color. As is well known, the ganglion cells in the retinas of a wide variety of animals exhibit nontrivial color opponency. This opponency is actually coupled to spatio-temporal opponency. For example, in primates at high background luminosities the most common type of ganglion cell has a receptive field consisting of a red center with green surround or a green center with red surround [4]. We shall call these cells 'single opponency' cells. What makes the color encoding problem even more challenging from a theoretical point of view is that the details of the chromatic and spatiotemporal interaction are not the same in all species. For example, the ganglion cells of goldfish and carp are quite different from those in monkeys and humans and exhibit what is termed "double opponency" between the red and green [5]. There are two types that are most common, one (type O in [5]) has a receptive field with red-green opponency in the center and the reverse opponency in the surround. The other (type Q) has

non-opponent red and green in the center with the reverse in the surround.

Below we shall see how the observed nontrivial interaction between color and space-time arises (due essentially to the presence of noise) even when the autocorrelator of natural scenes has no coupling between color and space-time. We will also find that this theory accounts for both single as well as double opponency and thus explains the color coding in retinas of organims as different as monkeys and fish. This happens because the theory leads to a family of solutions parametrized by the matrix elements (actually there are only two independent parameters in the red-green system) of the color correlation matrix. The single and double opponency cells turn out to be the two extremes corresponding to high and low correlation between the red and green cones, respectively. Since in primates, the spectral sensitivity peaks of the red and green cones are very close (separated by only $\sim$ 30 nm), high correlation between the red and green cone activities is expected which leads to the prediction of single opponency. While in the goldfish, where the peaks are separated by about 90 nm, the correlation is expected to be small leading to the prediction of double opponency.

We should point out that the earliest attempt to explain color opponency in the retina from the efficient encoding point of view was made by Buchsbaum and Gottschalk [6], who were also inspired by Barlow's [3] redundancy reduction hypothesis. However, their work included neither the spatial nor temporal dimensions, nor the noise. As we shall see below, color opponency cannot be explained without properly solving the problem in the realistic context of space-time and properly accounting for the noise.

The organization of the paper is as follows. In chapter one, we start by applying the measure of efficiency of ref. [2] to the case when the retinal encoding includes color. We then compute the various quantities appearing in that measure in terms of the statistical properties of the ensemble of visual messages. This measure of efficiency is subsequently used to explicitly derive the spatio-temporal-chromatic retinal transfer function. The predictions of the theory are finally compared with

experiment. An explication of the theory is not given here, rather the reader should refer to ref. [2].

2. Theory of spatio-temporal-chromatic encoding

A. Efficiency measure

In species that possess color vision, there are several distinct types of cones in the retina. For example, in humans and monkeys there are three types often termed "red", "green" and "blue". These cones differ from each other in the spectral absorption properties of their photo-sensitive molecules. For example, in humans the so called red cone is most sensitive to light at wavelength of about 558 nm, while the green and blue have peak spectral sensitivities near 530 nm and 419 nm, respectively [7] (the corresponding values for the macaque are 567, 535 and 440 nm [8]). The sensitivity of any given cone type to different light wavelengths has been measured extensively and is given by the spectral sensitivity function of that cone type, which we shall denote by $C^a(\lambda)$, where λ is the spectral wavelength and $a = 1, 2, 3$ stands for red, green and blue respectively. These functions for the monkey *Macaca fascicularis* are shown in Fig. 1 (very similar to those in humans). In the retina of humans and monkeys, the red and green cones are most abundant while the blue cones are rare [9]. Moreover, in the fovea the blue cones are almost nonexistent. Therefore we start by ignoring the blue cones and consider a system where only red and green cones exist at each sampling site. This is sufficient to give a good description of color vision in the fovea. We next show how the blue can be introduced as a perturbation to the red-green system and hence complete our description for parafoveal color vision. The rarity of the blue cones should clearly justify such an approach.

With this in mind, we can follow schematically what happens to a signal $s(\underline{x}, t, \lambda)$ falling on the retina, Fig. 2. First, the signal is filtered by the red and green cones (for completeness we have in Fig. 2 also included the blue cones but

used dashed lines to emphasize that the blue system does not exist at each sampling site) at each sampling site to produce the photoreceptors signals $L^1(\underline{x},t), L^2(\underline{x},t)$:

$$L^a(\underline{x},t) = \int d\lambda C^a(\lambda) s(\underline{x},t,\lambda) + \nu^a(\underline{x},t) \tag{2.1}$$

(with $a = 1,2$), where we have denoted the photoreceptor noise by $\nu^a(\underline{x},t)$. The chromatic and spatiotemporal signal $L^a(\underline{x},t)$ is subsequently linearly encoded by the ganglion transfer matrix to produce the ganglion output which is transmitted down the *output channel* or the optic nerve. In this red-green system we assume that the encoding does not change the dimensionality of the color space and hence we have two types of ganglion cells which we denote by the superscript $a = 1,2$. The linear encoding of these ganglion cells is

$$o^a(\underline{x}_n,t) = \sum_b \int d\underline{x}' dt' A^{ab}(\underline{x}_n,t;\underline{x}',t') L^b(\underline{x}',t') + \delta^a(\underline{x}_n,t), \tag{2.2}$$

where $o^a(\underline{x}_n,t)$ is the output of ganglion cell of type a whose receptive field is centered about $\underline{x}_n$ on the retina and $\delta^a(\underline{x}_n,t)$ is the output noise. The transfer matrix $A^{ab}(\underline{x}_n,t;\underline{x}',t')$, in addition to being a matrix in space-time, is a 2×2 matrix in color space. The notation used below is the same as in ref. [2], with boldfaced upper (lower) case quantities denoting matrices (vectors) in space-time. In addition, in this paper we use the convention that hatted quantities denote matrices (or vectors) in color space. So a boldface upper-case hatted quantity will stand for a matrix in color as well as space-time *e.g.* $\hat{\mathbf{A}}$ is $A^{ab}(\underline{x},t;\underline{x}',t')$.

We now apply the theory of visual processing of refs. [1,2], to derive $\hat{\mathbf{A}}$. The theory states that the purpose of the retinal encoding in all dimensions, space, time and even color, is to produce the most efficient representation of the incoming visual information. The appropriate measure of efficiency is the generalized redundancy

$$\mathcal{R} = 1 - I(\mathrm{O},\mathrm{S})/C \tag{2.3}$$

where $I(\mathrm{O},\mathrm{S})$ is the mutual information [10] or equivalently the amount of information in the ganglion cell outputs $o^a(\underline{x},t)$ about the ideal signal $s^a(\underline{x},t)$, and O

and S are the ensembles of all possible ganglion cell output $\hat{\mathbf{o}}$ and photoreceptor input signals, $\hat{\mathbf{s}}$, respectively. C in (2.3) is the capacity of the smallest channel that can carry the signal $o^a(\underline{x}, t)$ (see more precise definition below).

The efficiency measure $\mathcal{R}$ is a statistical measure that depends on the ensemble properties of the visual messages. For example

$$I(\mathrm{O},\mathrm{S}) = \sum_{\hat{\mathbf{o}},\hat{\mathbf{s}}} P(\hat{\mathbf{o}},\hat{\mathbf{s}}) \log\left[\frac{P(\hat{\mathbf{o}},\hat{\mathbf{s}})}{P(\hat{\mathbf{o}})P(\hat{\mathbf{s}})}\right],$$

where $P(\hat{\mathbf{s}})$ $(P(\hat{\mathbf{o}}))$ is the probability distribution of the ideal signal $\hat{\mathbf{s}}$ (ganglion outputs $\hat{\mathbf{o}}$), and $P(\hat{\mathbf{s}},\hat{\mathbf{o}})$ is the joint probability of $\hat{\mathbf{s}}$ and $\hat{\mathbf{o}}$. These probabilities are all computable upon knowledge of the statistical properties of S and of the noises $\boldsymbol{\nu}$ and $\hat{\boldsymbol{\delta}}$. We identify the ensemble S with the the ensemble of natural scenes in color (see ref. [2] for a more detailed discussion about the ensemble of natural scenes). In the case of linear encoding, one can argue that the most relevant statistical property is the two point correlator or autocorrelator of natural images [2]. In the context of color the autocorrelator is also a 2×2 matrix in color space, which we denote by $R^{ab}(\underline{x}, t; \underline{x}', t')$. This is defined as

$$R^{ab}_{ss}(\underline{x}, t; \underline{x}', t') \equiv \int d\lambda d\lambda' C^a(\lambda) C^b(\lambda') \left\langle s(\underline{x}, t, \lambda) s(\underline{x}', t', \lambda') \right\rangle,$$

where the expectation value $\langle\ \rangle$ denotes the standard information theoretic average.

Knowledge of $\hat{\mathbf{R}}_{ss}$ allows us to write $P(\hat{\mathbf{s}})$, as

$$\begin{aligned} P(\hat{\mathbf{s}}) = {} & [(2\pi)^{2V} \det \hat{\mathbf{R}}_{ss}]^{-1/2} \\ & exp[-\frac{1}{2}(\hat{\mathbf{s}} - \bar{\mathbf{s}}) \cdot \hat{\mathbf{R}}^{-1}_{ss} \cdot (\hat{\mathbf{s}} - \bar{\mathbf{s}})], \end{aligned} \tag{2.4}$$

which is the unique probability distribution, consistent with the autocorrelator being $\hat{\mathbf{R}}_{ss}$, and which maximizes the information $H(\mathrm{S}) = -\sum_{\hat{\mathbf{s}} \in S} P(\hat{\mathbf{s}}) \log P(\hat{\mathbf{s}})$ (see ref. [2]). In (2.4), we have included the mean of the signal $\bar{\mathbf{s}}$ although in our

analysis below it drops out and we have denoted the volume of space-time by V. For simplicity we represent the noise sources $\hat{\boldsymbol{\nu}}$ and $\hat{\boldsymbol{\delta}}$ by gaussian sources with variances $R_N^{ab} = N_a^2\delta^{a,b}$ and $N_\delta^2\delta^{a,b}$ respectively, where $\delta^{a,b}$ is the kronecker delta function (as we discuss below the homogeneity of the optic nerve fibers suggests that there is little variation in the output noise variance among fibers). Both sources of noise will be assumed not to have any significant correlations with the signal $\hat{\mathbf{s}}$. Given (2.4) and these assumptions about the noise, it is not difficult to show that the mutual information $I(\mathrm{O},\mathrm{S})$ is

$$I(\mathrm{O},\mathrm{S}) = \frac{1}{2}\log\frac{\det[\hat{\mathbf{A}}\cdot(\hat{\mathbf{R}}_{ss}+\hat{\mathbf{R}}_N)\cdot\hat{\mathbf{A}}^T + N_\delta^2\mathbf{1}]}{\det[\hat{\mathbf{A}}\cdot\hat{\mathbf{R}}_N\cdot\hat{\mathbf{A}}^T + N_\delta^2\mathbf{1}]}, \tag{2.5}$$

where the determinants are taken over space-time and color. In this form, the mutual information is a straightforward generalization of expression (2.7) in ref. [2].

In calculating the capacity C, we face some new issues when the color dimension is added. It is helpful before we examine these issues to review some of the discussion in [2] and spell-out more explicitly what C means. In ref. [2], C was defined as

$$C = \max_{P(\hat{\mathbf{w}})} I(\mathrm{O};\mathrm{W})\Big|_{\langle\hat{\mathbf{o}}^2\rangle=const.} \tag{2.6}$$

where $\hat{\mathbf{w}}$ is a dummy variable representing the input to the output channel and the maximization over $P(\hat{\mathbf{w}})$ is done for a given output variance $\langle o^a(\underline{\mathrm{x}},t)o^a(\underline{\mathrm{x}},t)\rangle$. Following analysis similar to that in [2], C can be written explicitly:

$$C = \frac{1}{2}\log\prod_{i,a}\left[\frac{\mathbf{A}\cdot(\mathbf{R}_{ss}+\mathbf{R}_N)\cdot\mathbf{A}^T + N_\delta^2\mathbf{1}}{N_\delta^2\mathbf{1}}\right]_{ii}^{aa}. \tag{2.7}$$

In this equation, the quantity $[\hat{\mathbf{A}}\cdot(\hat{\mathbf{R}}_{ss}+\hat{\mathbf{R}}_N)\cdot\hat{\mathbf{A}}^T + N_\delta^2\mathbf{1}]/N_\delta^2\mathbf{1}]_{ii}^{aa}$, is the variance (actually square of the variance) of the output in the fiber connected to the ganglion cell with color index a, at location i.

One way to think about C, (2.7), is that it is the capacity of the smallest channel that can carry the signal $\hat{\mathbf{o}}$ (with variance $\langle \hat{\mathbf{o}}^2 \rangle$). Thus C defined in (2.6) is not in general the capacity of the optic nerve, if by that we mean the absolute maximum amount of information that the optic nerve can ever transmit. The capacity of the optic nerve is equal to C only when (2.7) is evaluated at the highest signal variances allowed by the fixed dynamical range of the optic nerve fibers. At very high luminosities, where the incoming visual information is highest and the signal variances $\langle \hat{\mathbf{o}}^2 \rangle$ are highest, C coincides with the optic nerve capacity. At other adaptation levels, it is smaller and is the capacity of the smallest channel that could replace the optic nerve and still be able to transmit the signal $\hat{\mathbf{o}}$. In the next section we solve for the encoding $\hat{\mathbf{A}}$ that gives the smallest $\mathcal{R}$ by actually minimizing C, given a constraint on the amount of information preserved. In general this yields a set of minimal output variances $\langle \hat{\mathbf{o}}^2 \rangle$ which allow the information to be maintained. The underlying assumption here is that there is an advantage to the animal in minimizing this C at all adaptation levels. However, as we argue next, this benefit is not the same at all levels of adaptation.

At high background luminosities, the smallest C is also the smallest optic nerve capacity that can maintain the information. This smallest optic nerve capacity then gives a set of minimal nerve fiber dynamical ranges. The reason minimal dynamical range is advantageous to an animal is because the size of the fibers (diameter) grows with their dynamical range [11], which is believed to be a cost to the animal. At lower adaptation levels, minimizing (2.7) cannot be used to lower the physical size of the optic nerve fibers but has another very important benefit: An encoding that lowers C (2.7), is still one that packs the information in signals $\hat{\mathbf{o}}$ so they could fit into the smallest possible channel. Since we do not allow loss of useful information (see next section), the only way to force this information into effectively smaller channels is to squeeze out the noise as much as possible before transmission, again a benefit to the animal.

We are now ready to discuss the new issue that arises with the introduction of color. In general, an encoding $\hat{\mathbf{A}}$ leads to outputs which have different variances

for different fibers. In the purely spatiotemporal problem addressed in [2], this possibility did not arise because of the assumption of translation invariance of $\mathbf{A}$ and $\mathbf{R}_{ss}$, since then all terms in (2.7), for all the nerve fibers i, are equal. With color there is no theoretical reason to discount the possibility of different output variances among ganglion cells with different color index a. However, the anatomical evidence suggests that the optic nerve fiber sizes (in monkey) are unimodally distributed (see *e.g.* [12]) *i.e.* there is no evidence that the optic nerve fibers (at least the parvocellular portion of it) are grouped into collections of fibers with different dynamical ranges or fundamentally different properties. Now, if the nerve fibers have the same dynamical range, C in (2.7) is the optic nerve capacity at high luminosity only when the variances are all equal and set by the dynamical range of the nerve fiber. This implies that the most efficient encoding* distributes the output variances equally so as to utilize all the available dynamical range on every fiber, which leads to the constraint

$$(\hat{\mathbf{A}} \cdot (\hat{\mathbf{R}}_{ss} + \hat{\mathbf{R}}_N) \cdot \hat{\mathbf{A}}^T)^{11} = (\hat{\mathbf{A}} \cdot (\hat{\mathbf{R}}_{ss} + \hat{\mathbf{R}}_N) \cdot \hat{\mathbf{A}}^T)^{22}. \tag{2.8}$$

The analog of this constraint in space-time is automatically satisfied by our choice of translationally invariant $\hat{\mathbf{A}}$.

The constraint (2.8) has definitely to be imposed on $\hat{\mathbf{A}}$ at high luminosities, which is the regime most relevant to color vision. However, at low luminosities, where the transition to the rod system takes place, a constraint of the form (2.8) is not harmful since the outputs in the different color channels become degenerate. In this paper we examine color vision at high adaptation levels and examine the

---

$\star$ The argument goes as follows: In general the minimal capacity occurs for encodings that yield different variances on different fibers, which can be taken advantage of by choosing fibers with different dynamical ranges. However, if the fibers can only occur in one type with one value of dynamical range, what then is the most efficient way to transmit signals? If the signals o_a $(a = 1, n)$ are to be transmitted on separate fibers without "multiplexing" then the signal with the largest variance will set the size of all the fibers because only one type of fiber is available. Thus the capacity of the channel needed is $C = n \log(\max_a \langle o_a^2 \rangle)$. Using the mathematical fact that $n \log \max_a \langle o_a^2 \rangle \geq \sum_a \log \langle o_a^2 \rangle$ (where $\langle o_a^2 \rangle \geq 1$), with equality when all $\langle o_a^2 \rangle$ are equal, we see that the minimum C occurs when $\langle o_a^2 \rangle$ are all equal.

regime where the transition to the rod system occurs, both regimes where we are confident that (2.8) is valid. It is still to be seen whether this constraint is valid at intermediate luminosities.

We can now write the capacity C as

$$C = 2V \log \left[\mathrm{Tr}(\hat{\mathbf{A}} \cdot (\hat{\mathbf{R}}_{ss} + \hat{\mathbf{R}}_N) \cdot \hat{\mathbf{A}}^T / 2V N_\delta^2) + 1 \right], \tag{2.9}$$

subject to the constraint (2.8), which is a much simpler quantity to use than is (2.7).

B. A variational principle for $\mathbf{A}^{ab}$

According to the measure $\mathcal{R}$, (2.3), the most efficient encoding occurs when C and $I(\mathrm{O},\mathrm{S})$ are as close to each other as possible. This gives a design principle for $\mathbf{A}^{ab}$ and thus for the retina. As discussed in [2], one way to solve for $\mathbf{A}^{ab}$ is to minimize the functional

$$E\{\mathbf{A}^{ab}, \rho\} = C - \rho[I(\mathrm{O};\mathrm{S}) - I(\mathrm{L};\mathrm{S}) + \epsilon] \tag{2.10}$$

with respect to $\mathbf{A}^{ab}$ and the the lagrange multiplier ρ (we use ρ, instead of the λ used in ref. [2], to avoid confusion with the spectral wavelength λ). The latter enforces the constraint that no substantial amount of information should be lost in the process of recoding. $I(\mathrm{L},\mathrm{S})$ is the amount of information prior to the encoding and ϵ is a small positive number characterizing the small loss of information allowed. Some loss is inevitable due to the presence of the output noise $\boldsymbol{\delta}$. The amount of information in the photoreceptor signals, $I(\mathrm{L},\mathrm{S})$, is explicitly given by $\log\left[\det(\hat{\mathbf{R}}_{ss} + \hat{\mathbf{R}}_N)/\det\hat{\mathbf{R}}_N\right]$. It is not hard to see that this information diminishes as the amount of correlations between the cone activities increases and also as the noise levels N_a increase. A significant source of correlations in the color problem comes from the fact that the red and green spectral sampling mechanisms overlap highly and thus the activities of the red and green cones are expected to be highly correlated (see Fig. 1). This correlation causes further inefficiency [2] in the representation of the information at the level of the cones (see also [6])).

In (2.10) we can replace C by $\mathrm{Tr}\left[\hat{\mathbf{A}}\cdot(\hat{\mathbf{R}}_{ss}+\hat{\mathbf{R}}_N)\cdot\hat{\mathbf{A}}^T\right]/N_\delta^2$, keeping in mind that we always work subject to (2.8). The functional (2.10) then takes the following explicit form*

$$\begin{aligned}E\{\hat{\mathbf{A}},\rho\} =&\frac{1}{N_\delta^2}\,\mathrm{Tr}\left[\hat{\mathbf{A}}\cdot(\hat{\mathbf{R}}_{ss}+\hat{\mathbf{R}}_N)\cdot\hat{\mathbf{A}}^T\right]\\ &-\rho\left[\frac{1}{2}\log\frac{\det[\hat{\mathbf{A}}\cdot(\hat{\mathbf{R}}_{ss}+\hat{\mathbf{R}}_N)\cdot\hat{\mathbf{A}}^T+N_\delta^2\mathbf{1}]}{\det[\hat{\mathbf{A}}\cdot\hat{\mathbf{R}}_N\cdot\hat{\mathbf{A}}^T+N_\delta^2\mathbf{1}]}-I(\mathrm{L};\mathrm{S})+\epsilon\right].\end{aligned}\tag{2.11}$$

It is more convenient to redefine the matrix $\hat{\mathbf{A}}$

$$\hat{\mathbf{A}}'\equiv\hat{\mathbf{A}}\cdot\hat{\mathbf{R}}_N^{1/2}\cdot\hat{\mathbf{U}}_c,\tag{2.12}$$

where $\hat{\mathbf{R}}_N^{1/2}$ is the square root of the diagonal noise matrix $\hat{\mathbf{R}}_N$ and $\hat{\mathbf{U}}_c$ is the matrix that diagonalizes $\hat{\mathbf{R}}_N^{-1/2}\cdot\hat{\mathbf{R}}_{ss}\cdot\hat{\mathbf{R}}_N^{-1/2}$, *i.e.*

$$\hat{\mathbf{U}}_c^T\cdot\hat{\mathbf{R}}_N^{-1/2}\cdot\hat{\mathbf{R}}_{ss}\cdot\hat{\mathbf{R}}_N^{-1/2}\cdot\hat{\mathbf{U}}_c\equiv\hat{\mathbf{R}}'_{ss}=\begin{pmatrix}\mathbf{R}_+ & 0\\ 0 & \mathbf{R}_-\end{pmatrix}.\tag{2.13}$$

In terms of the redefined transfer matrix $\hat{\mathbf{A}}'$, the functional $E\{\hat{\mathbf{A}}',\rho\}$ takes a particularly simple form and correspondingly the variational equations $\partial E\{\hat{\mathbf{A}}',\rho\}/\partial\hat{\mathbf{A}}'$ are more tractable. Since we will be looking for translationally invariant solutions $A^{ab}(\underline{\mathrm{x}},t;\underline{\mathrm{x}}',t')=A^{ab}(\underline{\mathrm{x}}-\underline{\mathrm{x}}';t-t')$ we can go to frequency space through the standard fourier transform. For example, the fourier transform of the color correlation function is defined as

$$\mathrm{R}_{ss}^{ab}(\underline{\mathrm{k}},w)=\int d\underline{\mathrm{x}}dt e^{-i\underline{\mathrm{k}}\cdot\underline{\mathrm{x}}-iwt}\mathrm{R}_{ss}^{ab}(\underline{\mathrm{x}},t),$$

with a similar expression for $A^{ab}(\underline{\mathrm{k}},w)$. It is not difficult to show that the variational equations $\partial E\{A'^{ab},\rho\}/\partial A'^{ab}(\underline{\mathrm{k}},w)=0$, suppressing the $\underline{\mathrm{k}},w$ indices take

* The functional E has a symmetry $\hat{\mathbf{A}}\rightarrow\hat{\mathbf{U}}\cdot\hat{\mathbf{A}}$ where $\hat{\mathbf{U}}$ is an orthogonal matrix. Correspondingly, the solution, $\hat{\mathbf{A}}$, of $\partial E/\partial\hat{\mathbf{A}}=0$ will be fixed up to an orthogonal transformation. Imposing the constraint (2.8), then chooses a unique orthogonal transformation.

the simple form

$$\hat{A}' \cdot \left[(\hat{R}'_{ss} + 1) - \frac{\rho}{2} \left[((\hat{R}'_{ss} + 1) \cdot \hat{F} + 1)^{-1} \cdot (\hat{R}'_{ss} + 1) - (\hat{F} + 1)^{-1} \right] \right] = 0, \quad (2.14)$$

where all the objects appearing are 2×2 matrices in color space and $\hat{F}(\underline{k}, w)$ is the bilinear matrix $\hat{A}'^{T}(\underline{k}, w) \cdot \hat{A}'(\underline{k}, w)/N_f^2$. When $\hat{A}'(\underline{k}, w)$, as a function of $(\underline{k}, w)$ is non vanishing, the term inside the square bracket has to vanish. Thus

$$\left[\hat{F}(\underline{k}, w) + 1 \right] \left[\left(\hat{R}'_{ss}(\underline{k}, w) + 1 \right) \cdot \hat{F}(\underline{k}, w) + 1 \right] = \frac{\rho}{2} \hat{R}'_{ss}(\underline{k}, w) \cdot (\hat{R}'_{ss}(\underline{k}, w) + 1)^{-1}. \quad (2.15)$$

Since $\hat{R}'_{ss}(\underline{k}, w)$ is a diagonal matrix in color space given in (2.13), we can see from (2.15) that the solution for $F(\underline{k}, w)$ has to be diagonal with diagonal components $F_+(\underline{k}, w)$ and $F_-(\underline{k}, w)$. When $F_\pm$ are nonvanishing, they satisfy equations identical to (2.15) with $\hat{R}'_{ss}(\underline{k}, w)$ replaced by $R_+(\underline{k}, w)$ and $R_-(\underline{k}, w)$, respectively. The solutions are

$$F_\pm(\underline{k}, w) = \begin{cases} \dfrac{1}{2} \dfrac{R_\pm(\underline{k}, w)}{R_\pm(\underline{k}, w) + 1} \left(1 + \sqrt{1 + \dfrac{2\rho}{R_\pm(\underline{k}, w)}} \right) - 1, & \text{if } F_\pm > 0, \\ 0, & \text{otherwise.} \end{cases} \quad (2.16)$$

The correlators $R_\pm(\underline{k}, w)$ are explicitly given by

$$R_\pm(\underline{k}, w) = \frac{1}{2N_1^2 N_2^2} \Big[N_2^2 R_{ss}^{11}(\underline{k}, w) + N_1^2 R_{ss}^{22}(\underline{k}, w) \pm \left[\left(N_2^2 R_{ss}^{11}(\underline{k}, w) - N_1^2 R_{ss}^{22}(\underline{k}, w) \right)^2 + 4 N_1^2 N_2^2 \left(R_{ss}^{12}(\underline{k}, w) \right)^2 \right]^{1/2} \Big]. \quad (2.17)$$

The right hand side of the expression in (2.16) is identical to that in the pure space-time problem (see eq. 2.15 in [2]), except that the auto-correlator is replaced by R_+ and R_- for F_+ and F_- respectively. What this means is that introducing color leads to two decoupled space-time problems with effective autocorrelators

R_+ and R_- given explicitly in terms of the components of the spatiotemporal and chromatic correlator $R^{ab}_{ss}(\underline{k}, w)$ by (2.17). This fact will play an important role in our discussion below on the properties of the solution.

To recover the transfer matrix $\hat{A}$ we need to factorize $\hat{F}$ into $\hat{A}'^T$ and $\hat{A}'$ and then invert the change of variables in (2.12). Since $\hat{A}'$ is fixed up to multiplication by a 2×2 orthogonal matrix (recall $\hat{F} = \hat{A}'^T \hat{A}'/N_\delta^2$), we can go to a basis where $\hat{A}'$ is diagonal. In this basis, we have

$$\begin{pmatrix} F_+ & 0 \\ 0 & F_- \end{pmatrix} = \begin{pmatrix} A_l A_l^*/N_\delta^2 & 0 \\ 0 & A_c A_c^*/N_\delta^2 \end{pmatrix}$$

where A_l, A_c are the two diagonal components of $\hat{A}'$. The solutions for A_l and A_c are then given by $N_\delta\sqrt{F_+}$ and $N_\delta\sqrt{F_-}$, respectively, apart from phase factors that depend on $(\underline{k}, w)$. The dependence of these phase factors on w is fixed by the requirement of causality (see [2]), while the dependence on $\underline{k}$ is eliminated entirely by the requirement of rotation symmetry is space. (Actually there is still the freedom to multiply $\hat{A}'$ by ± 1 which leads to a degeneracy that can be identified with the *on* and *off* channels in the retina.) Since, in this paper we will be comparing the solutions with experiments that measured spatial properties at given temporal frequencies, it is not necessary to know the phase. Thus we can recover $\hat{A}_l$ and $\hat{A}_c$ simply by taking the square root of $F_\pm$. For the general case, the procedure described in section C.2 in [2] has to be used to extract the causal solutions. This finally leads to

$$\hat{A} = \hat{U}_\theta \cdot \begin{pmatrix} \sqrt{F_+} & 0 \\ 0 & \sqrt{F_-} \end{pmatrix} \cdot \hat{U}_c \cdot \begin{pmatrix} N_\delta/N_1 & 0 \\ 0 & N_\delta/N_2 \end{pmatrix} \tag{2.18}$$

where $\hat{U}_\theta$ is an as yet unspecified 2×2 orthogonal matrix. The matrix $\hat{U}_c(\underline{k}, w)$, defined in (2.13) is explicitly

$$\hat{U}_c(\underline{k}, w) = \begin{pmatrix} R^{12}_{ss}(\underline{k}, w)/D_+ & N_1 N_2 \left(R_+(\underline{k}, w) - R^{11}_{ss}(\underline{k}, w)/N_1^2\right)/D_+ \\ R^{12}_{ss}(\underline{k}, w)/D_- & N_1 N_2 \left(R_-(\underline{k}, w) - R^{11}_{ss}(\underline{k}, w)/N_1^2\right)/D_- \end{pmatrix},$$

where the denominators $D_\pm$ are given by

$$D_\pm = \left[\left(R_{ss}^{12}(\underline{k}, w) \right)^2 + N_1 N_2 \left(R_\pm(\underline{k}, w) - R_{ss}^{11}(\underline{k}, w)/N_1^2 \right)^2 \right]^{1/2}. \tag{2.19}$$

From among the family of solutions for $\hat{A}$ we still need to pick up the solution that satisfies the constraint (2.8). This uniquely fixes the orthogonal matrix $\hat{U}_\theta$ to be a rotation by the angle $\theta = \pi/4$ (the other allowed choices for $\hat{U}_\theta$ give the same solutions up to a trivial interchange of the red-green and/or interchange of on-off channels.)

To complete the solution, we need also to solve for ρ from the information preservation constraint. It can be shown straightforwardly that the equation for ρ simplifies to

$$\int d\underline{k} dw \left[\sum_{a \in \{+,-\}, F_a > 0} \log \left(\sqrt{\frac{R_a}{2\rho}} + \sqrt{1 + \frac{R_a}{2\rho}} \right) + \frac{1}{2} \sum_{a \in \{+,-\}, F_a = 0} \log(R_a + 1) \right] = \epsilon. \tag{2.20}$$

Generally, this equation is solved numerically for ρ.

C. Properties of the solution

The theory of optimal encoding gives a definite expression for $\hat{A}$, (2.18). Before we can exhibit $\hat{A}$ explicitly, however we must have a knowledge of the chromatic-spatio-temporal correlator $R_{ss}^{ab}(\underline{k}, w)$. This correlator, unfortunately, has not been measured yet, but we have some constraints on what it may be from the measurements in space [13] and from earlier work [2]. Also, some of the most important phenomena we exhibit here, such as the interaction between color opponency and spatio-temporal opponencies, do not depend on the detailed form of R_{ss}^{ab}. The simplest approach then is to assume that $R^{ab}(\underline{x}, t; \underline{x}', t')$ factorizes into the spatiotemporal correlator $R_{ss}(\underline{x}, t; \underline{x}', t')$, used in ref. [2], (and which Field [13] measured in the spatial domain), and a chromatic correlation matrix R_c^{ab}. In the frequency

domain this is

$$R_{ss}^{ab}(\underline{k}, w) = R_c^{ab} \times R_{ss}(\underline{k}, w) \tag{2.21}$$

where R_c^{ab} is a matrix of numbers given by the convolutions

$$R_c^{ab} = \int d\lambda d\lambda' C^a(\lambda) C^b(\lambda') R_c(\lambda, \lambda'), \tag{2.22}$$

where $R_c(\lambda, \lambda')$ is the spectral correlation function of natural scenes (at the same spatio-temporal point).

In the analysis below, we study the form of the solution in various limits for the choice of color correlation matrix elements R_c^{ab}. Actually, since an overall scale from R_c^{ab} can be absorbed in the definition of the signal in $R_{ss}(\underline{k}, w)$, there are only two independent parameters in the symmetric matrix R_c^{ab}. In what follows, we set $R_c^{11} = 1.0$, so we are left with R_c^{12} and R_c^{22}. The spatio-temporal correlator $R_{ss}(\underline{k}, w)$ is explicitly the same as that used in the purely spatiotemporal analysis [2], namely

$$R_{ss}(\underline{k}, w) = S^2 \frac{1}{(\underline{k}^2 + w^2 + \mu^2)^{3/2}} e^{-2(\underline{k}^2 + w^2)^{1/2}/\kappa_c} \tag{2.23}$$

where S^2 is the signal strength, μ is the reciprocal of the receptive field size of the cell, and κ_c is the acuity scale (about 18 c/deg for monkeys and humans).

To get some insight into the solution (2.18) we, for simplicity, set the noise variances equal: $N_1 = N_2 \equiv N$. In this case R_+ and R_-, (2.17), are given by the product of the eigenvalues of the color matrix R_c^{ab} times the spatiotemporal correlator $R_{ss}(\underline{k}, w)/N^2$:

$$R_{\pm}(\underline{k}, w) = r_{\pm}(\frac{S}{N})^2 R_{ss}(\underline{k}, w)$$

where $r_{\pm}$ are the eigenvalues (numbers) of R_c^{ab}, and we have explicitly exhibited the S^2 factor in $R_{ss}(\underline{k}, w)$. Consequently, the two effective space-time problems, that the full problem decomposes into, have solutions (2.16) which are identical

to those encountered in the pure space-time problem except now the S/N ratios involved are multiplied by the eigenvalues of the color matrix R_c^{ab}: $(S/N)_l^2 = r_+(S/N)^2$ and $(S/N)_c^2 = r_-(S/N)^2$. In many species, especially humans and monkeys, the spectral sensitivity profiles highly overlap, see Fig. 1. On average the distance between the red and green spectral sensitivity peaks is only about 30 nm in primates. This means that the matrix R_c^{ab} is expected to have components which are numerically close to each other, with the red and green highly correlated. If we examine the limit $R_c^{12} \sim R_c^{22} \sim$ O(1), then the color correlation matrix possess a hierarchy in its eigenvalues. One eigenvalue, r_+, will be relatively large and corresponds essentially to the eigenvector (red+green) or $R + G$, which can be called the *luminance* channel and the other, r_-, will be relatively small and corresponds essentially to $R - G$, which can be called the *chromatic* channel.

The effective signal to noises $(S/N)_{l,c}^2 = (S/N)^2 r_\pm$ in the corresponding space-time problems will also have a hierarchy, $(S/N)_l/(S/N)_c >> 1$ regardless of what S/N is. From the space-time problem we know what the profiles in (2.16), or actually the A_l and A_c profiles look like as a function of signal to noise. For the high signal to noise $(S/N)_l$, A_l will exhibit spatio-temporal opponencies and perform contrast detection, while A_c corresponding to the low $(S/N)_c$, will merely perform smoothing. In the frequency domain this is equivalent to the statement that A_l and A_c will be a band-pass and a low-pass filters, respectively. This is demonstrated in Fig. $3A$, where we have plotted A_l and A_c for some set of parameters given in the caption. From this we see that the luminance channel A_l, where there is no color opponency, turns out to exhibit spatio-temporal opponencies, while for the chromatic channel A_c, where there is color opponency, exhibits no spatio-temporal opponencies. This is the origin of the coupling between space-time and color and is fundamentally related to the fact that noise exists, and that the system can improve its signal to noise in one domain (for example space) by integrating over another domain (color). This coupling could of course be accentuated if the original spatio-temporal chromatic correlator had couplings between color and space-time.

The chromatic and the luminance channels, however are not what get trans-

mitted down the optic nerve since the final matrix $\hat{A}$, (2.18), is a rotation by $\pi/4$ that superposes these two channels. This superposition of the luminance and the chromatic channels results, as we shall see below, in a channel of red-center with green-surround and another channel of green-center with red-surround. The intuitive reason for this "multiplexing" is the fact that the amount of information in the luminance and chromatic channels is very different and thus these channels require fibers with different dynamical ranges (there is more information in the luminance channel and hence it requires fibers with larger dynamical ranges), while the physiological constraint (2.8) forces all fibers to essentially have the same properties. Therefore the retina multiplexes the information in these two channels in order to utilize most efficiently the available optic nerve fibers. Actually, later in the brain (where the brain can allocate regions of very different sizes to color and luminance) there is evidence that suggests that the information is reorganized again into luminance and chromatic channels (see [14,15]). It is interesting to see that the results of psychophysical contrast sensitivity experiments (Fig. $3B$) that essentially probe the luminance and the chromatic channels give curves that look similar to those in Fig. $3A$. In Fig. $3B$, it is clear that the red-green contrast sensitivity curve (solid triangles) is a low pass filter while the monochromatic, solid squares, (which mostly probes the properties of the luminance channel) is a band-pass filter.

D. Numerical calculations

We have numerically calculated the solution in (2.18), to exhibit what the function $A^{ab}(\underline{k}, w)$ looks like in various parameter regimes. Fig. 4 and Fig. 5 give this function and its fourier transform in space, respectively, for a limiting set of parameters where $R^{22} \approx R^{12} \sim \mathrm{O}(1)$ and at high S/N. The answer is not too sensitive to the actual choice of parameters as long as they are relatively close. As we can see from Fig. 5, this gives one cell which has predominantly red excitatory center and green inhibitory surround and another cell with green inhibitory center with red excitatory surround (of course there are also the cells with reverse polarity $\hat{\mathbf{A}} \rightarrow -\hat{\mathbf{A}}$). Ignoring the blue, these are the types of cells that Derrington et. al [4] find. From the contrast sensitivity curves we see that the first cell at low spatial

frequency performs $R-G$ opponency; however as the spatial frequency increases, the cell makes a transition to $R+G$ processing. This is also what Derrington et al. [4] find, in their experiments where they measured color opponency properties of ganglion cells as a function of spatial frequency. The location of the transition from $R-G$ to $R+G$ is predictable in terms of the elements of the color correlator.

Another feature predicted by the theory is a loss of color as the signal to noise goes down, since as S/N decreases the chromatic channel A_c becomes vanishingly small and only the luminance channel survives. Fig. 6 gives the contrast sensitivity at low signal to noise; both cells are performing $R+G$ processing at all frequencies. We interpret the point where the chromatic channel is lost as the point of transition to the rod system, *i.e.* at that point the retina does not need two sampled inputs (red and green cones), it only needs one sampling. We can also examine the answer as the temporal frequency of stimulation increases. In that case we also find a loss of color happening at a predictable temporal frequency. Better measurements of the autocorrelator of natural scenes would enable us to make concrete numerical predictions about when color loss happens and where the transition to the rod system happens, as a function of temporal frequency and signal to noise.

Fig. 4 is typical as long as the matrix elements of R_C^{ab} are close to each other, and clearly shows the single opponency cells that are found in experiments on monkeys. The question now is how can this theory account for the double opponency cells observed in goldfish and carp? [5]. One fact that turns out to be the clue to solving this problem is the location of the peak of the red sensitive cone in these species. In goldfish the red cone has a peak spectral sensitivity around 620 nm (in carp 611 nm) while the green cone is roughly about the same location as in monkeys and humans namely 530 nm (in carp 529 nm). Thus the red-green mechanisms are separated by about 90 nm instead of about 30 nm in primates. What this means is that the color correlation matrix will necessarily have off-diagonal components which are much smaller than the diagonal ones, *i.e.* $R_c^{12} << 1.0$. In the numerical integration of $\mathbf{A}^{ab}$, when we allow the off-diagonal (green-red coupling strength) components of R_c^{ab} to become small we get the typical curves shown in

Fig. 7. Without doubt these can be termed double opponency cells. In general the cells in different species will fall somewhere between the two extremes of single vs. double opponency. So all types of color opponency cells are related continuously by varying the off-diagonal component of the color correlator matrix.

As mentioned earlier, a significant fact here is that even when the autocorrelator of natural scenes does not have any coupling between space-time and color, the resulting retinal transfer function does. The underlying cause of such coupling is the noise in the photoreceptors and such a phenomena could not be understood by ignoring that noise. We should point out that one source that contributes to the noise in the photoreceptors is chromatic aberration. Better measurements of the correlation matrix and the noise characteristics in the cones will enable us to quantitatively assess whether chromatic aberration or other sources of noise (quantum, intrinsic etc.) control the details of the opponency observed.

Another point that should be mentioned here is that with color vision new possibilities are opened for retinal adaptation to gross properties of the background light. Rather than a single number L_0 describing the adaptation level, there may be different average luminosities for each of the photoreceptor types. That is, there may be adaptation to the background spectrum. It also may be possible for the photoreceptors themselves to change in sensitivity with varying conditions (see [16]). In either case, this type of adaptation manifests itself in our analysis as a change in the signal to noise ratios for each of the photoreceptors, which appear as numerical coefficients in the color matrix. This means that adapting to background spectrum is equivalent to changing the parameters in the color matrix. As a result, fascinating adaptations could in principle take place. However, the change in background spectrum from daylight to moonlight is not dramatic [17], so such adaptation may be small. Experiments to test spectral adaptation in ganglion cells would be a useful probe to explore the theory.

E. Introducing the Blue

So far we have ignored the blue cones in our calculations. As mentioned, this

is justified in the primate fovea where there are virtually no blue cones. It is also justified as a first approximation elsewhere in the retina since the blue cones are very sparsely distributed, as are ganglion cells with blue cone afferents. While this sparseness makes ignoring the blue cones a good approximation, it also complicates somewhat including the blue cones in the calculations. This is because the blue sampling is at a different spatial scale than the red and green sampling, so it is incorrect to take the correlation matrix as a direct product of a 3×3 color matrix times a single spatial autocorrelator. However, by a trick, we can get some idea of the type of additional solutions which arise when the blue cones are included. Instead of taking accurately into account the true spatial sampling of the blue cones, we take them to be as numerous as the other cones. But we then compensate for this fiction by choosing each of their signals to be only a fraction of the true signal of a blue cone. With this admittedly crude strategy, the analysis using a 3×3 color matrix times a single spatiotemporal autocorrelator, proceeds as above.

Including the blue cones differs from the red-green case in diagonalizing the color matrix, since now there will be three output channels rather than only the $R + G$ and $R - G$ channels. However, when the blue cone amplitudes are small and they correlate weakly with the other cones, as we are assuming, then the three channels in the diagonal basis consist of the old $R + G$ and $R - G$ plus a new $R + G - B$ channel. Recall that once we found solutions in the diagonal basis, we next had to rotate them in color space until the average ganglion outputs were equalized. But that step is only required when the ganglion cell fibers are equally numerous and of equal size, since otherwise it would be wasteful for them not to share the signals equally. However, since we are here treating blue cones on an equal footing only as a convenience, it would be incorrect to rotate the blue cone solutions to equalize their outputs with the others. In other words, our argument here is only self consistent if it results in a large number of very weak blue-sensitive outputs which can then be seen as an approximation to a small number of reasonably strong outputs: the inverse of the approximation made for the blue photoreceptors. The upshot is that we expect, as a perturbation of our above result,

a small number of ganglion cells whose color response is approximately $R+G-B$. Their spatiotemporal responses should also be the one expected for low S/N, since the S/N is proportional to the third color eigenvalue which is by assumption very small. This means a more lowpass type of response with a relatively lower spatial frequency cutoff, which is consistent with the data [4].

3. Summary

To summarize our results, we find that efficient encoding of the spatio-temporal-chromatic signals by the retina accounts for all the prominent features observed in color vision in various species:

1. In any retina with two cones with close spectral sensitivity peaks, such as the red and green cones in primates, the theory predicts a pair of ganglion cells: one with red center and green surround and one with green center and red surround, Fig. 5. In the frequency domain these predicted kernels make a transition from R-G at low frequency to R+G at high frequency, Fig. 4.

2. In any retina with two cones with distant spectral sensitivity peaks, such as the red and green cones in goldfish, the theory predicts a pair of double opponency ganglion cells: one with R-G center and G-R surround and one with R+G center and -R-G surround, Fig. 7.

In deriving results 1 and 2, we find that the theory makes two important predictions: first that spatio-temporal and color information is organized into luminance and chromatic channels, and second that these are multiplexed for most efficient transmission through the optic nerve.

3. Independent of the color correlation matrix, as adaptation level decreases, the predicted solutions become more low pass and start to loose color discriminability. At the lowest levels, all solutions become sensitive only to luminance signals, which we interpret as a transition to the rod system, Fig. 6.

4. If a third cone type (blue) is added sparsely, as in primates, a heuristic argument predicts a relatively smaller number of ganglion cells with $B - (R + G)$ opponency in color and with lowpass filtering in space-time.

5. The theory shows that the luminance channel performs band pass filtering while the chromatic channel performs low pass filtering, Fig. $3A$, which agrees with the psychophysical contrast sensitivity experiments, Fig. $3B$. The theoretical coupling between color and space-time properties comes from the fact that the effective space-time signal to noise in the chromatic channel is multiplied by the smaller ("R-G") eigenvalue of the color matrix, while the luminance signal to noise is multiplied by the larger ("R+G") eigenvalue.

Acknowledgements

We would like to thank F. Dyson, J. Krauskopf and L. Maloney for useful discussion and the Seaver Institute for its support.

Figure Captions

Fig. 1

The spectral sensitivity curves $C^1(\lambda), C^2(\lambda)$ and $C^3(\lambda)$ for the red, green and blue cones respectively, for the monkey *Macaca fascicularis*. The curves are all exactly the same shape, but differ in the location of their peaks and they were calculated from the standard data for constructing the absorbance spectrum of any visual pigment, based on retinal and of known peak spectral sensitivity (see for e.g. ref. [7]).

Fig. 2

Schematic diagram showing the stages of transformations undergone by an ideal signal $s(\underline{x}, t, \lambda)$ falling on the surface of the retina. In the first stage, the photoreceptors sample this signal both chromatically and in space-time to produce the photoreceptor signal L^a (a=1,2,3 corresponding to red, green and blue). This signal is then recoded linearly by the ganglion cells to produce the output o^a which is transmitted down the optic nerve. The noise at the photoreceptor stage is denoted by ν^a while the output noise is δ^a. We have used dashed lines to distinguish the cells that receives blue afferents (which are rare) from those in the red-green system.

Figs. $3A, B$

A. The calculated chromatic (low-pass) and luminance (band-pass) channels for single cells. The parameters are in the limiting case of $R_c^{22} = 1.0$ and $R_c^{12} = 0.995$, and $S/N = 4.0$, $\mu = 0.2$ and $\epsilon = .2$. The band-pass and low-pass curves exist over a very wide range of parameters. The parameters chosen here represent an extreme where disparity between the two channels is accentuated.

B. Psychophysical contrast sensitivity as a function of spatial frequency for a red-green grating, solid squares, and a green monochromatic grating, solid triangles, drawn from the data of Mullen [15]. The solid squares probe the

properties of the chromatic channel while the solid triangles essentially probe properties of the luminance channel. This statement is not precise since the true chromatic and luminance channels are not exactly $R - G$ and $R + G$ channels, however the point here is that the data does support two channels with low-pass and high-pass properties.

Fig. 4

The chromatic transfer function (equivalently contrast sensitivity curves) A^{ab} as a function of spatial frequency, in the limit when the matrix elements of the color correlator are close to each other. The solid lines denote positive (excitatory) values while the dashed lines are negative (inhibitory). Note that at low frequencies the ganglion cell of type 1, top two graphs, has an $R - G$ opponency while at high frequency it makes the transition to $R + G$ processing, with a similar phenomena for the second cell type 2. This transition was seen in the experiments in [4]. The curves were generated for the limiting values $R^{22} = 0.999$ and $R^{12} = 0.9$ and $S/N = 40.0$, $\mu = 1.0$, $\epsilon = 1.0$. The S/N, μ and ϵ values are typical values for the monkey [2] at high luminosity, while the values for R_c^{ab} are chosen to represent the extreme limit of high correlation of the red and green cone activities. The curves qualitatively look the same for a wide range of values for R_c^{ab} as long as R_c^{12} remains a significant fraction, more than about 30% of R_c^{22} (recall R_c^{11} is by convention set to 1).

Fig. 5

The chromatic transfer function A^{ab} as a function of the distance from the center of the cell in units of μ^{-1}. Since the transfer function is rotationally symmetric we have projected the answer down to one dimension by integrating it over one direction. The curves are also calculated at a fixed and very small temporal frequency. The parameters used are the same as those in the caption of Fig. 4. Note that the two types of cells are red center with a green surround and a green center with a red surround, which is what is found in

[4] for the monkey.

Fig. 6

The effect of lowering S/N (equivalently the overall background luminosity) on the chromatic transfer function A^{ab} exhibited in spatial frequency space, at a fixed temporal frequency. The solid lines denote positive (excitatory) values while the dashed lines are negative (inhibitory). The parameters used are the same as those in the caption of Fig. 4 except that S/N is now 1.0 instead of 40.0. We can see that the two types of cells perform $R+G$ type of processing at all spatial frequencies. A similar behavior is seen as the temporal frequency is increased even when S/N is kept constant and high.

Fig. 7

The chromatic transfer matrix in the regime where the red-green cone activities are not significantly correlated. The parameters used are $R_C^{22} = 0.5$ and $R_c^{12} = 0.05$, $S/N = 40.0$, $\mu = 0.5$ (the receptive field size of fish is larger than that of monkey), $\epsilon = 1.0$. We see the double opponency very clearly in this limit, the first cell type has red excitatory with green inhibitory center and red inhibitory and green excitatory surround. This cell type corresponds to type O cells found by Daw [5] in the goldfish retina. The other cell type has a red and green inhibitory center with a red and green excitatory surround. This corresponds to type Q cells in [5].

REFERENCES

1. Atick, J. J., and Redlich, A. N., " Towards a theory of early visual processing". Neural Comp. **2**, 308-320 (1990).

2. Atick, J. J., and Redlich, A. N., "Quantitative tests of a theory of retinal processing: Contrast sensitivity curves". Preprint no. IASSNS-HEP-90/51, Oct. 1990.

3. Barlow, H. B., "Possible principles underlying the transformation of sensory messages". In *Sensory Communication*, W. A. Rosenblith, ed. M.I.T. Press, Cambridge, MA (1961).

4. Derrington, A. M., Krauskopf, J. and Lennie, P. "Chromatic mechanisms in lateral geniculate nucleus of macaque". J. Physiol. **357**, 241-265 (1984).

5. Daw, N. W. "Colour-coded ganglion cells in the goldfish retina: Extension of their receptive fields by means of new stimuli". J. Physiol. **197**, 567-592 (1968).

6. Buchsbaum, G. and Gottschalk, A. "Trichromacy, opponent colours coding and optimum colour information transmission in the retina". Proc. R. Soc. Lond. **B 220**, 89-113 (1983).

7. Dartnall, H. J. A., Bowmaker, J. K. and Mollon, J. D. " Microspectrophotometry of human photoreceptors". In *Colour vision*, Mollon, J. D. and Sharpe, L. T. eds. Academic Press, London (1983).

8. Bowmaker, J. K., Dartnall, H. J. A. and Mollon, J. D. "Microspectrophotometric demonstration of four classes of photoreceptor in an Old World primate, *Macaca fascicularis*". J. Physiol. **298**, 131-143 (1980).

9. De Monasterio, F. M., McCrane, E. P., Newlander, J. K. and Schein, S. J., "Density profile of blue-sensitive cones along the horizontal meridian of macaque retina. Invest. Ophthalmol. Vis. Sci., **26**, 289-302 (1985).

10. Shannon, C. E. and Weaver, W., *The Mathematical Theory of Communication.* The University of Illinois Press, Urbana (1949).

11. Levick, W. R., "Sampling of information space by retinal ganglion cells". In *Visual Neuroscience.* Pettigrew, J. D., Sanderson, K. J. and Levick, W. R., eds. Cambridge University Press. Cambridge (1986).

12. Hughes, A. "New perspectives in retinal organisation". Prog. in retinal research, vol. **4**, 243-312 (1985).

13. Field, D. J., "Relations between the statistics of natural images and the response properties of cortical cells". J. Opt. Soc. Am. A **4**, 2379-2394 (1987).

14. Krauskopf, J., Williams, D. R. and Heeley, D. W., "Cardinal directions of color space". Vis. Res. **22**, 1123-1131 (1982).

15. Mullen, K. T. ."The contrast sensitivity of human colour vision to red-green and blue-yellow chromatic gratings". J. Physiol. **359**, 381-400 (1985).

16. Eisner, A. and Macleod, D. I. A., "Flicker photometric study of chromatic adaptation: Selective suppression of cone inputs by colored background". J. Opt. Soc. Am. **71**, 705-718 (1981).

17. Lythgoe, J. N., *The ecology of vision.* Oxford University Press. Oxford (1979)

Fig. 1

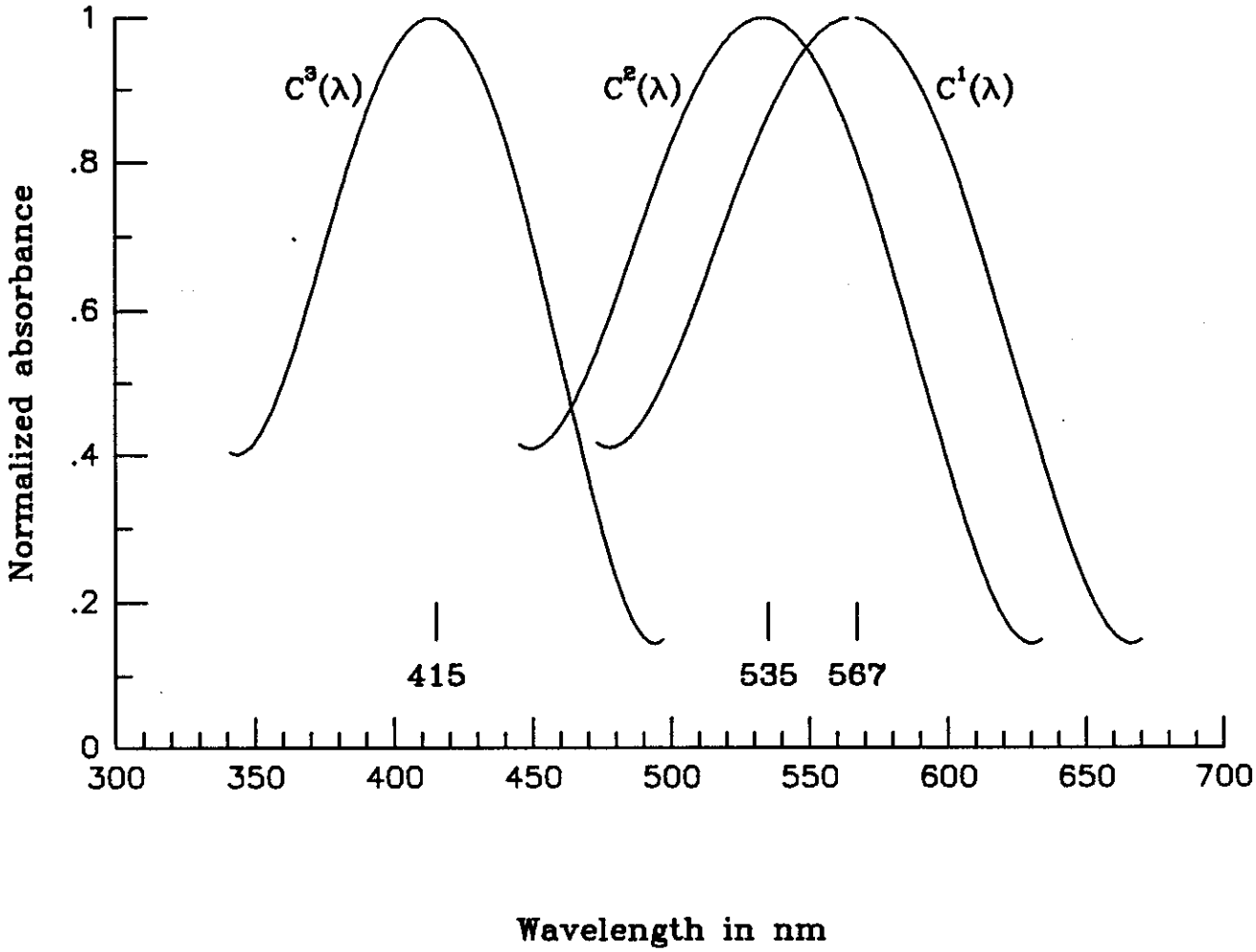
Normalized absorbance
1
.8
.6
.4
.2
0
300
350
400
450
500
550
600
650
700
C³(λ)
C²(λ)
C¹(λ)
415
535
567
Wavelength in nm

Fig. 2

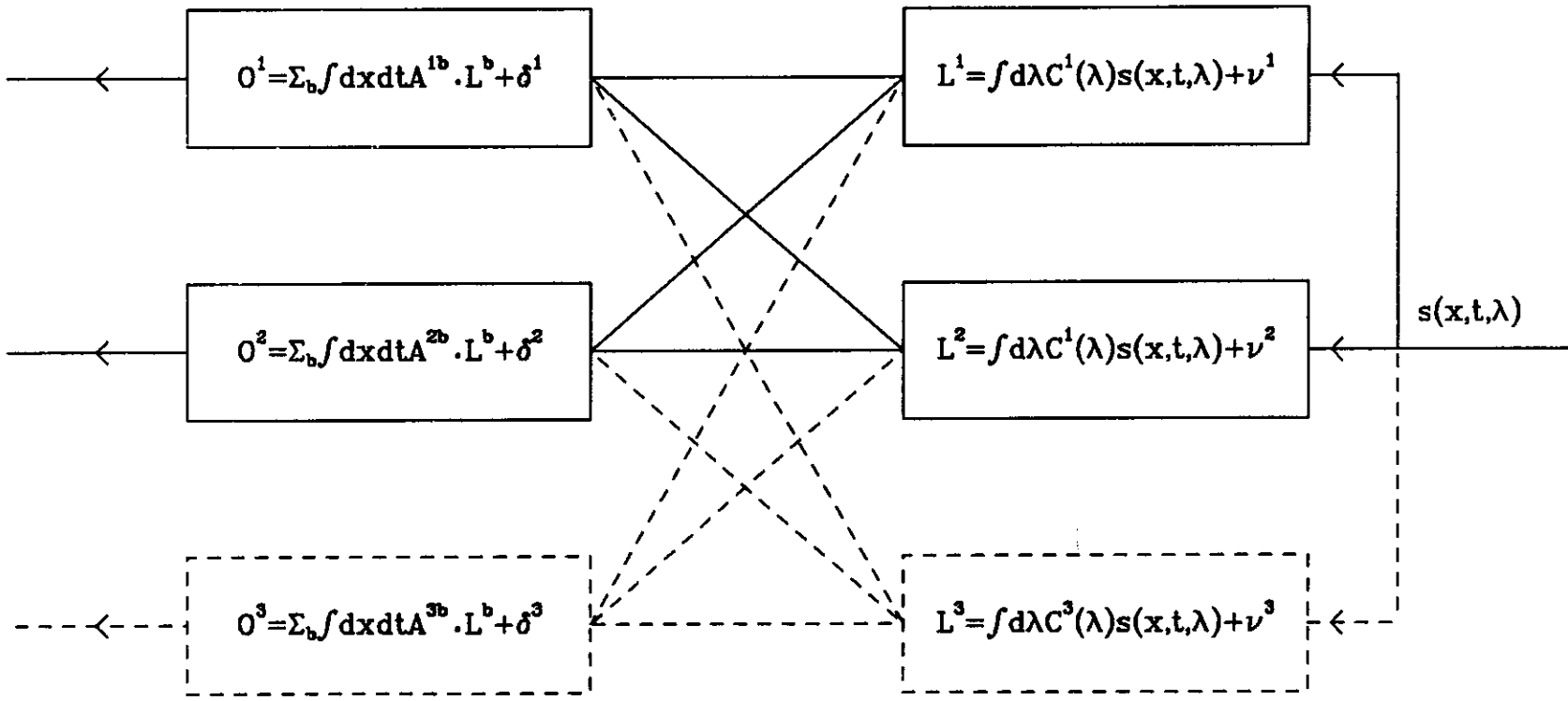
$O^1=\Sigma_b\int dxdtA^{1b}.L^b+\delta^1$
$O^2=\Sigma_b\int dxdtA^{2b}.L^b+\delta^2$
$O^3=\Sigma_b\int dxdtA^{3b}.L^b+\delta^3$
$L^1=\int d\lambda C^1(\lambda)s(x,t,\lambda)+\nu^1$
$L^2=\int d\lambda C^1(\lambda)s(x,t,\lambda)+\nu^2$
$L^3=\int d\lambda C^3(\lambda)s(x,t,\lambda)+\nu^3$
$s(x,t,\lambda)$
Optic nerve
Recoding
Photoreceptor sampling

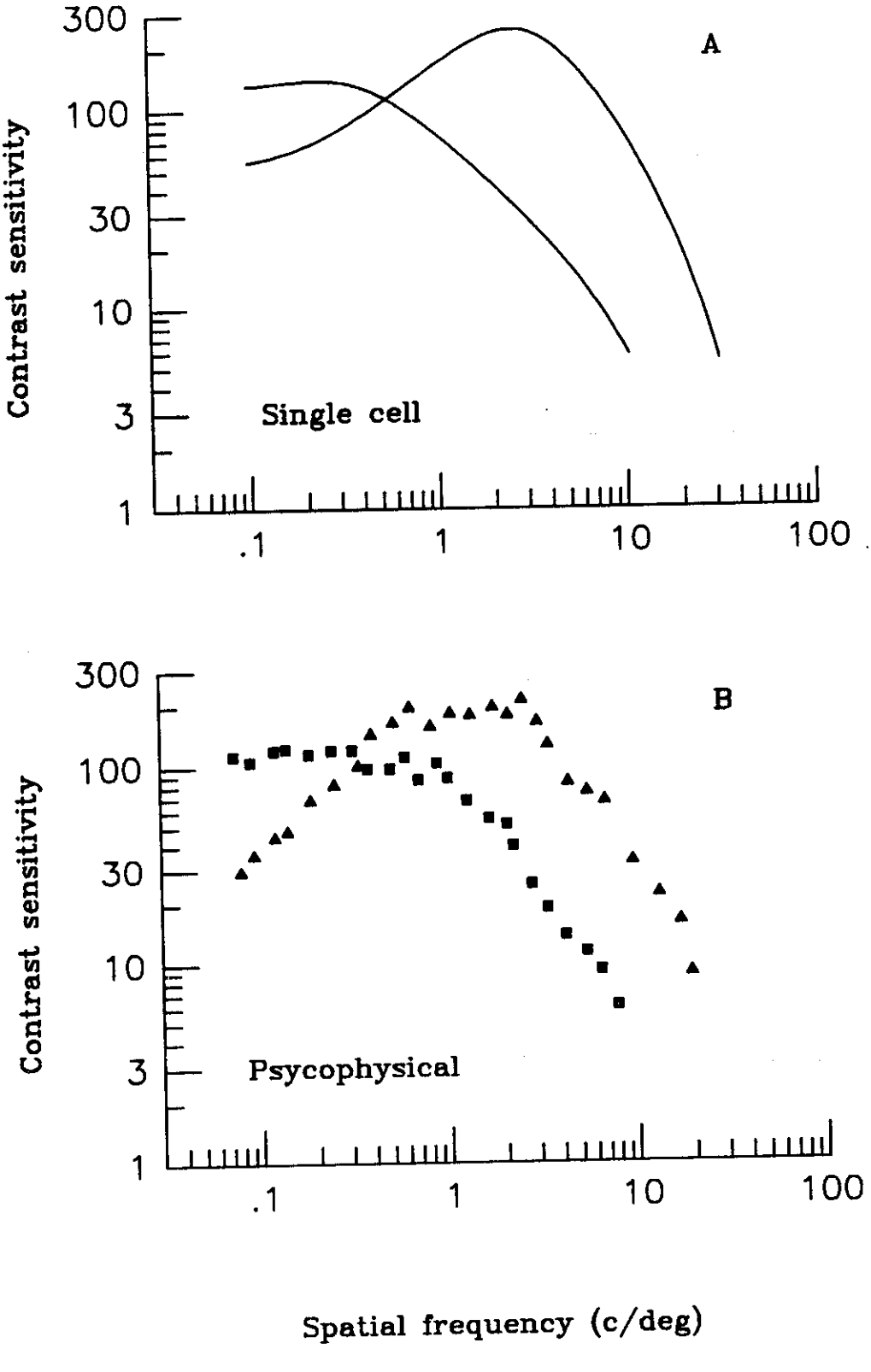
300
100
30
10
3
1
Contrast sensitivity
A
Single cell
.1
1
10
100
300
100
30
10
3
1
Contrast sensitivity
B
Psycophysical
.1
1
10
100
Spatial frequency (c/deg)

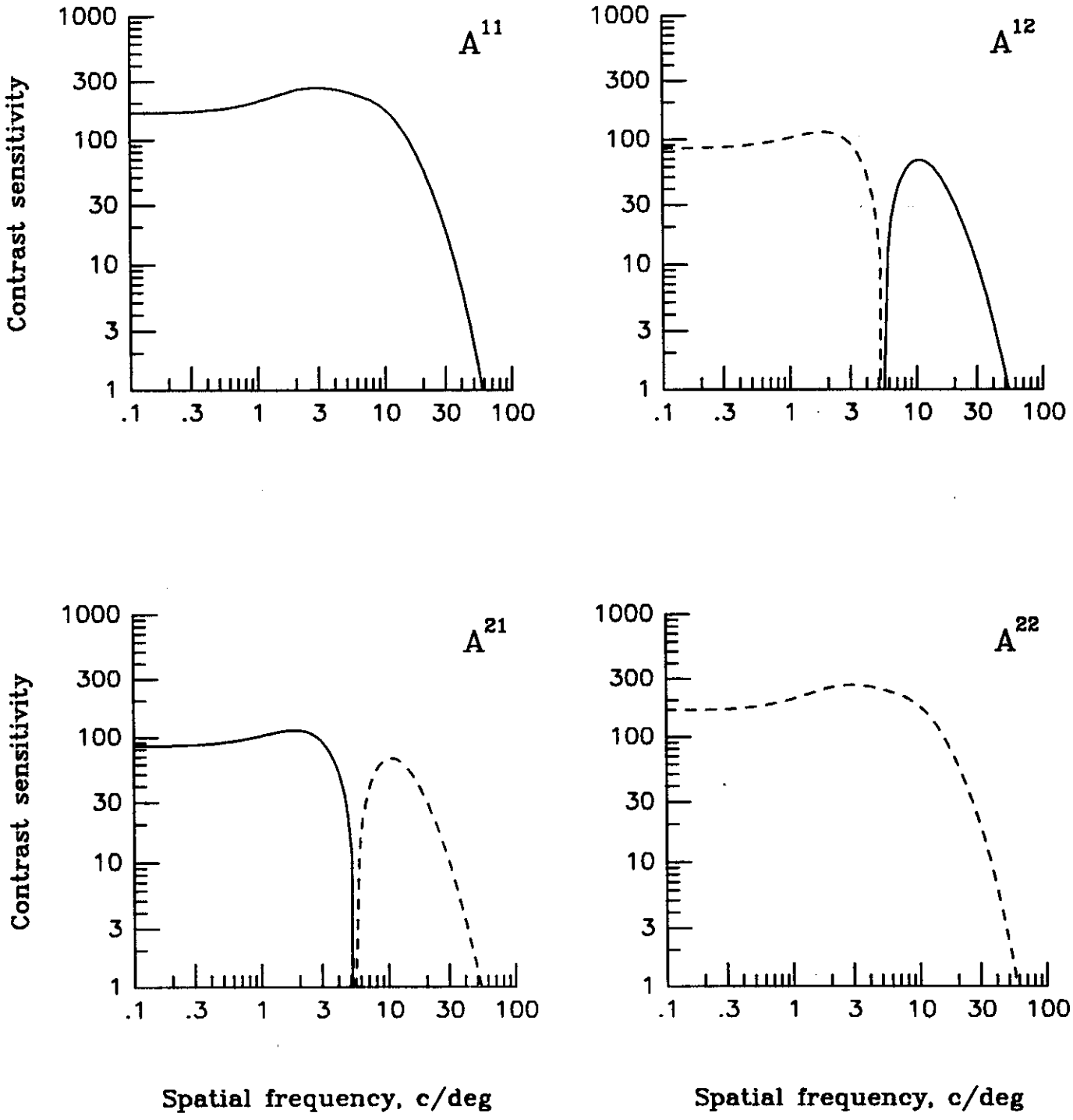
Contrast sensitivity
1000
300
100
30
10
3
1
.1
.3
1
3
10
30
100
A11
A12
A21
A22
Spatial frequency, c/deg
Spatial frequency, c/deg

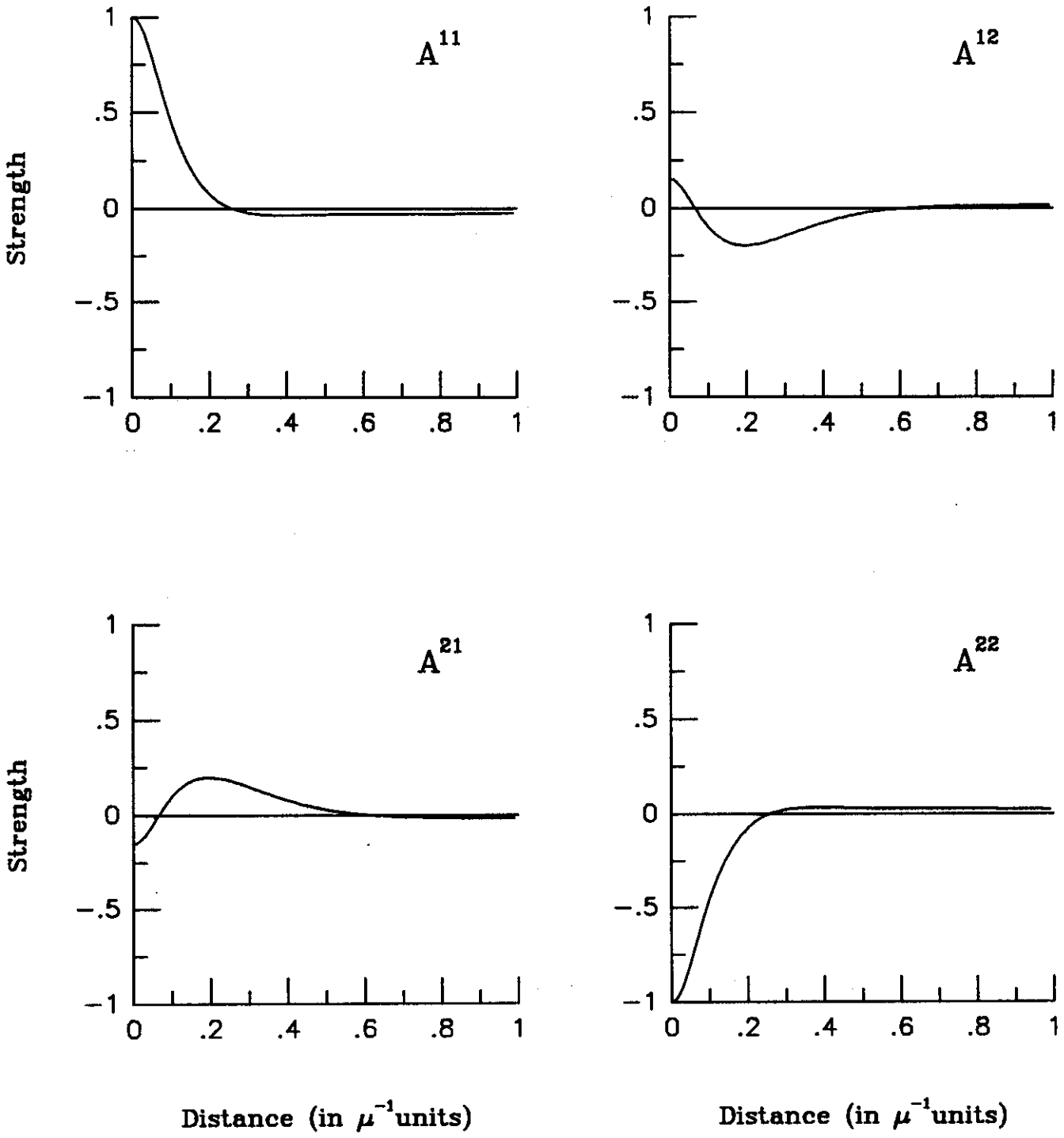
A11
A12
A21
A22
Strength
Strength
1
.5
0
−.5
−1
0
.2
.4
.6
.8
1
Distance (in μ^{-1}units)
Distance (in μ^{-1}units)

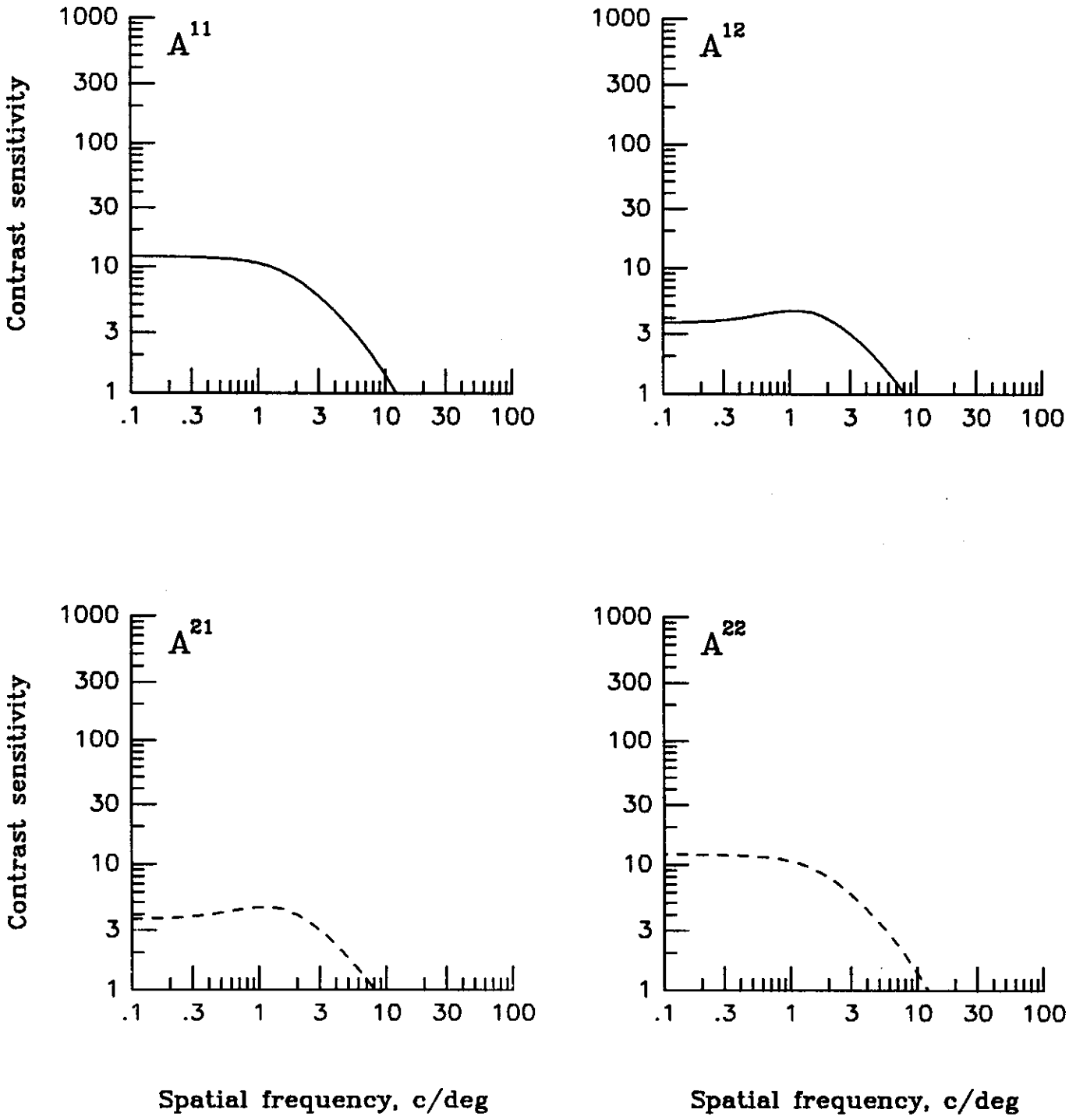
A11
A12
A21
A22
1000
300
100
30
10
3
1
.1
.3
1
3
10
30
100
Contrast sensitivity
Contrast sensitivity
Spatial frequency, c/deg
Spatial frequency, c/deg

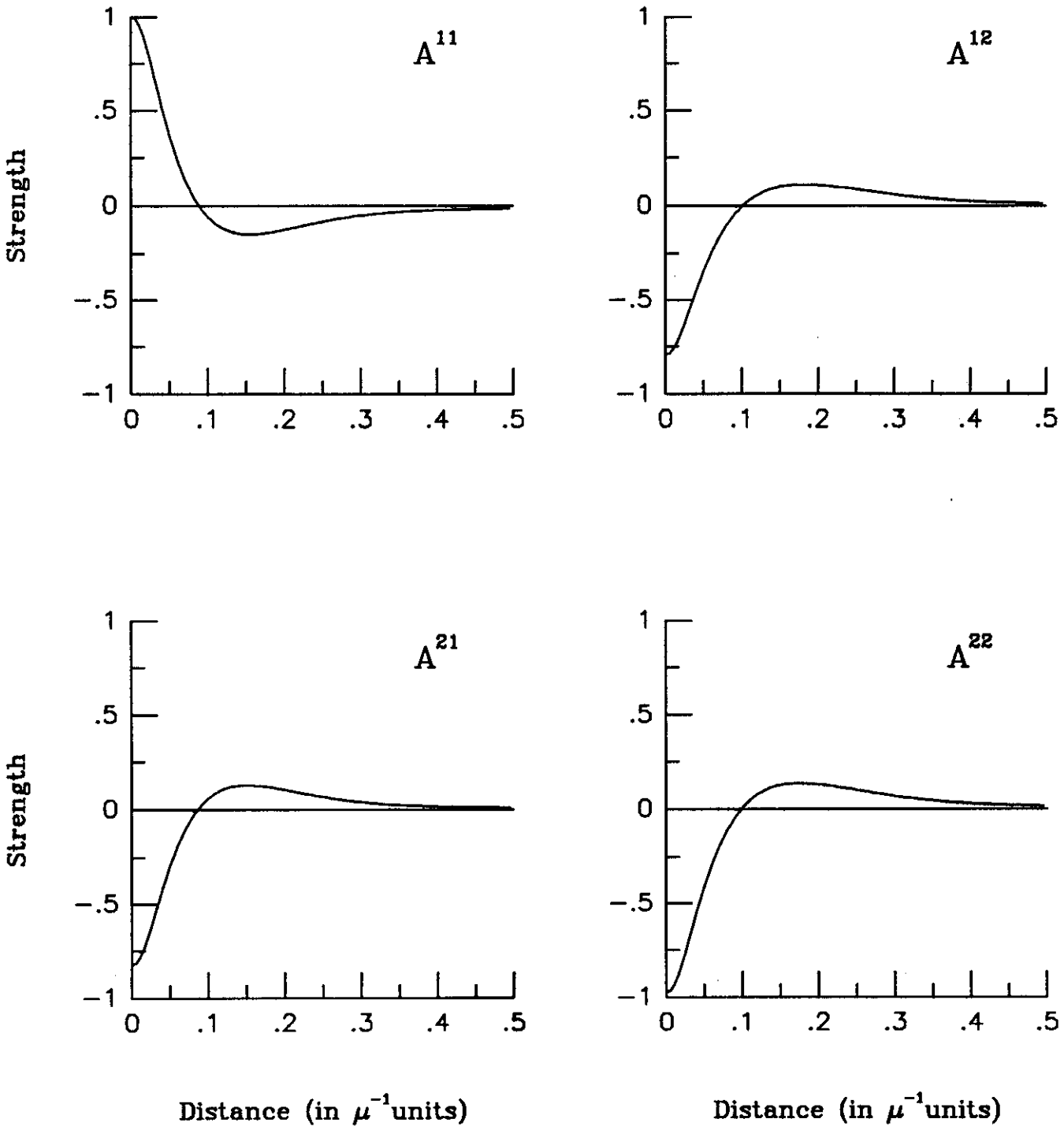
A11
A12
A21
A22
Strength
Strength
1
.5
0
−.5
−1
0
.1
.2
.3
.4
.5
Distance (in μ⁻¹units)
Distance (in μ⁻¹units)